



Sulforaphane Can Intensify The Antitumor Effect Of Gemcitabine By Targeting Cancer Stem Cells In Non-small Cell Lung Cancer Via Suppressing TGF- β 1/TNF- α Factor

Ibrahim A. Zahran,^{a*} Enas M. Moustafa,^b Manar S. Fouda,^a Fatma A. Salem,^a Mohamed M. Omran^a



CrossMark

^a Chemistry Department, Faculty of Science, Helwan University, Cairo, Egypt.

^b Radiation Biology Department, National Center for Radiation Research & Technology (NCRRT), Egyptian Atomic Energy Authority (EAEA), Cairo, Egypt.

Abstract

Cancer stem cells (CSCs) are cells in a malignancy that have the potential to self-renew and differentiate, resulting in a diverse population of cancer cells. These cells are increasingly linked to resistance to traditional therapies, as well as tumour recurrence. Sulforaphane (SFN), a strong anti-cancer and well-tolerated nutritional substance, reduces CSC characteristics and improves gemcitabine therapeutic effectiveness in the non-small cell lung cancer (NSCLC) rat model. Gemcitabine (GEM) and/or SFN enhance these capabilities by reducing transforming growth factor beta1 (TGF- β 1) and tumor necrosis factor alpha (TNF- α), which target CD133 and aldehyde dehydrogenase 1A1 (ALDH1A1) CSC markers. This discovery was supported further by changes in histological findings. Furthermore, we demonstrated that GEM and/or SFN had a highly substantial inhibitory effect on the viability of A549 cells. *In vitro*, combination treatment increased chemotherapeutic drug cytotoxicity. SFN sensitized NSCLC cells to GEM effectiveness, which was accompanied by suppression of GEM-induced CSC formation in lung cancer tissues according to the findings. GEM+SFN, a combination therapy, has demonstrated promising results in restricting the availability of CSCs, suggesting that it might be effective in combating NSCLC resistance and recurrence.

Keywords: Sulforaphane; Gemcitabine; NSCLC; CSCs; TGF- β ; TNF- α ; Combination therapy.

1. Introduction

Non-small cell lung cancer (NSCLC) is a leading cancer in terms of causing deaths among all cancers in the world, accounting for approximately 80% of all lung cancer cases [1]. Gemcitabine is a deoxycytidine nucleoside analog widely used for NSCLC treatment [2,3]. Gemcitabine has anti-proliferative properties which depend on blocking cell cycle progression at the G1/S transition and interrupt the synthesis of DNA [4]. Gemcitabine is recommended as the first-line chemotherapy for treatment of pancreatic cancer of advanced stage [5]. It is also used for treating NSCLC [2], bladder cancer [6], ovarian cancer [7] as well as breast cancer [6]. Gemcitabine is regarded as a perfect choice for evaluation as maintenance therapy due to its tolerability profile [8]. However,

gemcitabine resistance is one of the main obstacles to a successful treatment of cancer, which may be acquired or intrinsic. GEM has been reported to induce reactive oxygen species (ROS), the high level of which is cytotoxic whereas the low level may be tumor promoting [9,10]. Furthermore, metabolic reprogramming towards aerobic glycolysis can be induced by low-dose GEM, resulting in promotion of cancer stemness and chemoresistance in pancreatic cancer through activation of the KRAS (Kirsten rat sarcoma virus) /AMPK (AMP-activated protein kinase) pathway mediated by ROS [11].

Cancer stem cells are often linked to stem cell properties such as chemotherapy resistance, increased capacity of anchorage-independent growth,

*Corresponding author e-mail: ibrahimzahran@science.helwan.edu.eg

Receive Date: 10 April 2022, Revise Date: 17 May 2022, Accept Date: 19 May 2022

DOI: 10.21608/EJCHEM.2022.132222.5856

©2023 National Information and Documentation Center (NIDOC)

expression of stem cell antigens [12]. CSCs markers have been detected in many cancer types such as CD133, CD44 and ATP-binding cassette transporter G2 (ABCG2) [13]. The cell surface antigen CD133 has been found to be responsible for drug resistance, tumorigenicity, invasion, and metastasis [14]. Transforming growth factor beta is a cytokine family member that plays a role in regulation of cell proliferation [15, 16]. It seems to have a dual role in cancer where TGF- β 1 signaling can act as a tumor suppressor inhibiting cell proliferation in normal hematopoietic cells and epithelial cells [16–19]. Moreover, many tumors have been shown to evade immune system recognition via increasing TGF- β expression and, so, increasing tumor metastasis and recurrence risk [20]. The primary role of TNF- α is the stimulation of inflammatory cells to fight infection, whilst its proapoptotic capability is still ambiguous. Nevertheless, it is supposed that nuclear factor kappa B (NF- κ B), the main channel for TNF- α proinflammatory action, strongly inhibits TNF- α induction of apoptosis. TNF- α activates many antiapoptotic through regulation of both caspase and NF- κ B [21].

Crosstalk between TGF- β 1 and TNF- α promotes cancer stemness in breast cancer via epithelial-mesenchymal transition (EMT) induction. Especially, EMT-generated breast CSCs induced by TGF- β have a claudin-low phenotype that is normally linked to mesenchymal characteristics and more aggressive behavior of cancer, as well as self-renewal potential, increased *in vivo* tumorigenicity and resistance against the chemotherapy oxaliplatin [22]. TNF- α and TGF- β 1 were reported to be of the most abundant cytokines playing critical roles not only in enhancing invasion and migration abilities of cancer cells, in addition to promoting their stemness [23, 24].

Sulforaphane, a naturally derived isothiocyanate, has been found to be a potent histone deacetylase (HDAC) inhibitor as well as an enhancer of several pro-apoptotic signaling pathways. Recent studies indicated that SFN may inhibit the activity and expression of matrix metalloproteinases (MMPs) which are implied in regulating metastasis, and may inhibit CSCs activity [25,26]. However, little has been reported on the direct antitumor activities of SFN on NSCLC with the linkage of cancer cells assault and migration *in vivo*. Therefore, the current study highlights the anticancer and cytoprotective

effects of SFN in combination with GEM in order to overcome NSCLC resistance and recurrence.

2. Experimental

2.1. Chemicals

Urethane (ethyl carbamate), and Sulforaphane (SFN) were acquired from Sigma-Aldrich Chemical Co., St Louis, MO, USA and were of high purity, quality and analytical grade. Gemcitabine (2,2-difluorodeoxycytidine; GEM) was got in its commercial formula as Gemzar® (Lilly). All used chemicals were of the highest quality and analytical grade.

2.2. Cell culture

NSCLC A549 human cell line was attained from the Tissue Culture Unit of the Holding Company for Biological Products and Vaccines (VACSERA), Giza, Egypt, supplied through the American Type Culture Collection (ATCC).

2.3. Culture medium

The cells were cultured in RPMI-1640 medium in a humidified environment at a temperature of 37°C and 5% CO₂ atmosphere. The medium was supplemented with 100 IU/ml penicillin, 100 µg/ml streptomycin and 10% fetal bovine serum (FBS).

2.4. Subculture of cell line

Cultured cells were observed via an inverted microscope (CKX41; Olympus, Japan) to evaluate the confluence degree and to ensure the absence of bacterial and fungal contaminations. Phosphate-buffered saline (PBS) free of Ca²⁺/Mg²⁺ was used to wash the cell monolayer using a volume that is equivalent to the half of the culture medium volume. The cells were harvested by adding trypsin/EDTA using 1mL/25cm² of surface area. The flask was then got back into the incubator and left for 10 minutes. To ensure that all the cells were detached, the cells were examined by the inverted microscope.

2.5. Assay of sulforaphane (SFN) cytotoxicity

To investigate the cytotoxic effect of sulforaphane (SFN) on A549 NSCLC human cell line, the crystal violet assay was performed as previously described [27]. A549 NSCLC cells were plated onto 96-well culture plate and exposed to various concentrations of SFN (5, 10, 15, 25, 30 and 35 µM), in addition to untreated cells of A549 cell line that served as a control. The plate was incubated for 24 hours in a

humidified incubator at a temperature of 37°C and 5% CO₂ atmosphere. The medium was then aspirated at the end of the incubation period. The cells were washed using 100 µL of PBS. The MTT (3-[4,5-dimethylthiazol-2-yl]-2,5-diphenyl tetrazolium bromide) reagent was added (10 µL/well) and the culture plate was incubated for 12 hours allowing for the intracellular reduction of the soluble yellow MTT into the insoluble purple formazan crystals. Finally, the dye was extracted from the cells by the addition and mix of 33% acetic acid with each well content. The resulting colored solution was quantified by measuring the absorbance at 490 nm in triplicates using an ELISA reader (Stat Fax, USA). The cytotoxicity was assessed as the end point of crystal violet reduction and the quantitative external morphology of exposed cells in relation to control cells was assessed by an inverted microscope. The percentage of cell survival was calculated as the percentage of the ratio of the optical density (OD) as shown by the following equation: cell survival % = OD treated / OD control × 100.

2.6. Culture groups

The cultured A549 NSCLC cells were divided into four groups. Group 1 (positive control group) included untreated A549 cells that served as a positive control. Group 2 (GEM group) involved A549 cells treated with the IC₅₀ of GEM (0.01 µM) [28]. Group 3 (SFN group) included A549 cells treated with the IC₅₀ of SFN (30 µM). Group 4 (GEM+SFN group) included A549 cells treated with GEM and SFN.

2.7. Assay of cell proliferation

Cell proliferation of A549 NSCLC human cell line in all groups was evaluated using the MTT cell proliferation kit (Cat. No. 4890-25-K; Trevigen Inc., Gaithersburg, MD, USA) as provided by the manufacturer's protocol. Cells were plated in a 96-well microplate (10³-10⁵ cells/well) in the absence or presence of GEM (0.01 µM) and /or SFN (30 µM) in a total volume of 100 µL of cell culture medium and were then allowed to attach overnight. The MTT reagent was added (10 µL/well) and the culture plate

was incubated for 12 hours allowing for the intracellular reduction of the soluble yellow MTT into the insoluble purple formazan crystals. The detergent reagent was added to each well to solubilize the formazan crystals and the resulting colored solution was quantified by the measurement of each sample prior to at 550-600 nm by an ELISA reader. For each group, three wells were used. Cell proliferation was evaluated as the cell proliferation percentage compared to the untreated cancer cell line as a control.

2.8. Animals and experimental design

Female adult Wistar rats (n = 100, 120–150 g for each) were obtained from the animal breeding house of the National Center for Radiation Research and Technology (NCRRT). The animals had been adapted in the animal facility of NCRRT for at least one week before they were subjected to experimentation. The animals were retained under typical housing circumstances that involved a temperature of 23 ± 1 °C, relative humidity of 55 ± 5%, and a 12h:12h light-dark cycle. The rats were fed a commercial standard pellet diet (including necessary nutritive elements such as 23% protein, 4.68% fats and 2.6% fibers; and being soya free to minimize natural phytoestrogen supplementation) and were given water ad libitum. This study was carried out in compliance with the National Institute of Health's Guide for the Care and Use of Laboratory Animals (NIH Publication No. 85-23, revised 1996) as well as the NCRRT ethic committee's guidelines which approved all experimental procedures. The animals were divided at random into the following five groups (20 rats for each group):

Group 1 (Normal control): Normal rats.

Group 2 (NSCLC): Rats received three injections of urethane 1 g/kg body weight (BW) administered intraperitoneally at weekly intervals [29,30].

Group 3 (NSCLC+GEM): NSCLC rats were treated intraperitoneally with GEM at the week 21 and the week 22 with two doses per week (50 mg/kg BW) [31]. The twice weekly dosage of gemcitabine is equal to a 300 mg/m², the typical human low dose using the body surface area standardization formula.

Group 4 (NSCLC+SFN): NSCLC rats were treated orally at the week 21 with SFN (100 mg/kg BW, daily) [32] for 6 weeks.

Group 5 (NSCLC+GEM+SFN): NSCLC rats were treated with GEM and SFN as in group 3 and 4, respectively.

2.9. Blood and lung tissue sampling

By the end of the study, rats from the different groups were sacrificed by cervical dislocation, and the blood was collected by retro-orbital sinus puncture. Lungs were resected rapidly, washed with isotonic saline, and used for biochemical and other tests of lung tumorigenesis histopathological examination. All blood samples and lung specimens were stored at -80°C until analysis.

2.10. Assessment of oxidative stress

Lipid peroxidation in lung tissue was determined by thiobarbituric acid assay that involves the reaction between malondialdehyde (MDA) and thiobarbituric acid, forming the pink-colored complex thiobarbituric acid reactive substances (TBARS). The absorbance was measured at 532 nm [33]. Reduced glutathione (GSH) in lung tissue homogenate was assessed according to the method previously described by Ahmed et al., 1991 [34]. Superoxide dismutase (SOD) and catalase (CAT) activity were assayed in lung tissue homogenate in accord with the method designated by Minami & Yoshikawa, [35] and Sinha, [36], respectively.

2.11. Enzyme-linked immunosorbent assay (ELISA) analyses

The lung tissues were used for estimating the level of caspase-3 and TNF- α consistent with the manufacturer's protocol of rat ELISA kit obtained from MyBiosource, Inc. California, San Diego, USA (Cat. No. MBS743552 and Cat. No. MBS2507393, respectively). TGF- β 1 was measured by using rat TGF- β 1 ELISA kit purchased from CUSABIO Technology LLC, Houston, TX, USA (Cat. No. CSB-E04727r) as stated by the protocol provided by the manufacturer. Samples' measurements were carried out by an ELISA reader (Biotek, USA).

2.12. Gene expression analysis of CD133 and ALDH1A1 using quantitative real-time polymerase chain reaction (qRT-PCR)

Real-time PCR was performed using the StepOne Real-Time PCR System Instrument (Life Technologies) with reaction contained SYBR Green Master Mix (Applied Biosystems), gene-specific forward and reverse primers, cDNA synchronized from the extraction RNA (0.5-2) micrograms, and nuclease-free water. The sequences of PCR primer pairs used for each gene are shown in table 1. Data analysis have been carried out by the ABI Prism sequence detection system software and data quantification has been performed by means of the v1_7 Sequence Detection Software from PE Biosystems (Foster City, CA).

Table 1 Sequences of primers used for qRT-PCR

| Primer | Sequence |
|----------------|---|
| CD133 | Forward: 5'- TACAACGCCAAACCACGACTGT -3' Reverse: 5'- TCTGAACCAATGGAATTCAAGACCCTTT -3' |
| ALDH1A1 | Forward: 5'- TCGTCTGCTGCTGGCGACAA -3' Reverse: 5'- AGCCCAACCTGCACAGTAGCG -3' |
| β -actin | Forward: 5'- CCAAGGCCAACC GCGAGAAGATGAC -3' Reverse: 5'- AGGGTACATGGTGGTGCCGCCAGAC -3' |

The comparative threshold cycle approach was used to calculate the relative expression of the genes under study. All values were normalized to the β -actin gene, which was used as the housekeeping gene [37].

2.13. Histopathological examination

Lung tissue specimens from all animal groups were obtained and preserved in 10% neutral buffered formalin. The specimens were then trimmed, washed, and dehydrated in ascending concentrations of

alcohol, cleaned in xylene, embedded in paraffin, sectioned at 4-6 μ m thickness and stained with hematoxylin-eosin staining (H&E) according to Bancroft et al. [38]. The response of tumor mass to treatment was divided into the following: Grade I a, marginal or no regression; Grade I b, morphologic evidence of therapy-induced alterations but >10% residual tumor; Grade II a, extensive response but with residual tumor < 10%; and Grade II b, pathologic complete response [39].

2.14. Statistical analysis

All statistical analyses and graphs were carried out by GraphPad Prism 8.4.3 software (GraphPad Software, Inc., San Diego, CA, USA) and SPSS Statistics 19 software (IBM Corp., Armonk, NY, USA). Descriptive one-way analysis of variance (ANOVA) followed by Tukey's post hoc test and Pearson correlation test were used to calculate statistical significance. Results were presented as means \pm SD. Statistically significant p values are less than 0.05.

3. Results

3.1. Anticancer effect of different concentrations of SFN against A549 NSCLC human cell line

The cytotoxic activity of SFN against A549 NSCLC human cell line has been estimated via the MTT assay. The anticancer effects have been observed when cells were treated with increased concentrations of SFN (15 μ M to 35 μ M) showing the concentration 30 μ M as the half maximal inhibitory concentration (IC₅₀), as illustrated in figure 1.

3.2. Effects of GEM, SFN, and GEM+SFN on cell proliferation of A549 NSCLC human cell line

SFN and GEM as a combination therapy in group 4 manifested the most significant anticancer activity compared to either of SFN or GEM monotherapies, as presented in figure 1.

3.3. Effects of GEM, SFN, and GEM+SFN on oxidative status

To assess the oxidative status in the lung tissue following administration of GEM, SFN, and GEM+SFN, we measured the level of the lipid peroxide MDA, GSH, SOD activity and CAT activity in lung homogenates and our results are shown in figure 2. Our results have shown that treatment with SFN increased the lipid peroxide MDA ($p = 0.134$) as compared with NSCLC group. Furthermore, GEM and GEM+SFN therapies increased the lipid peroxide MDA to a highly significant extent ($p < 0.001$ for both). Treatment with GEM and GEM+SFN caused a decline in GSH level ($p = 0.343$ and $p = 0.768$, respectively) whereas treatment with SFN caused a rise in GSH level ($p = 0.878$) relative to NSCLC group.

Compared to NSCLC group, our results revealed a decrease in SOD activity in GEM treatment group (p

$= 0.983$), whilst the results revealed an increment in the activity of SOD in GEM+SFN treatment group ($p = 0.083$). Moreover, a significant raise in the activity of SOD was found in SFN treatment group ($p = 0.002$). In comparison with NSCLC group, our results exhibited a highly significant decrease in CAT activity in GEM treatment group ($p < 0.001$). Additionally, a significant elevation in the activity of CAT was exhibited in SFN treatment group ($p = 0.007$), at the same time that a modulated increase of the activity of CAT was exhibited in GEM+SFN treatment group ($p = 0.091$).

3.4. Effects of GEM, SFN, and GEM+SFN on caspase-3, TNF- α , and TGF- β 1

The level of caspase-3 in the NSCLC group was slightly increased compared to the normal control group ($p = 0.515$). Compared to the NSCLC group, caspase-3 levels showed an increase in both the GEM and SFN groups ($p = 0.163$ and $p = 0.610$, respectively). Additionally, a highly significant increase of caspase-3 has been manifested in the SFN+GEM combination therapy group ($p < 0.001$) as illustrated in figure 3a.

TGF- β 1 was found to be increased to a highly significant degree in the NSCLC group compared to the normal control group ($p < 0.001$). In comparison with the NSCLC group, the TGF- β 1 level was reduced in GEM, SFN, and SFN+GEM groups with a highly significant difference ($p < 0.001$ for all groups) (Fig. 3b). Our results also showed a highly significant increment of TNF- α in the NSCLC group compared to the normal control group ($p < 0.001$). TNF- α levels were lower in the SFN-treated group ($p = 0.053$) than these in the NSCLC group. Furthermore, TNF- α levels, compared to NSCLC group, were significantly lower in the GEM-treated group ($p = 0.004$). A highly significant reduction was seen in the GEM+SFN combination therapy group ($p < 0.001$) in comparison to the NSCLC group (Fig. 3c).

3.5. Effects of GEM, SFN, and GEM+SFN on the CSCs markers CD133 and ALDH1A1

Measurement of CD133 has demonstrated that CD133 was increased in NSCLC group to a highly significant extent compared to the normal control group ($p < 0.001$).

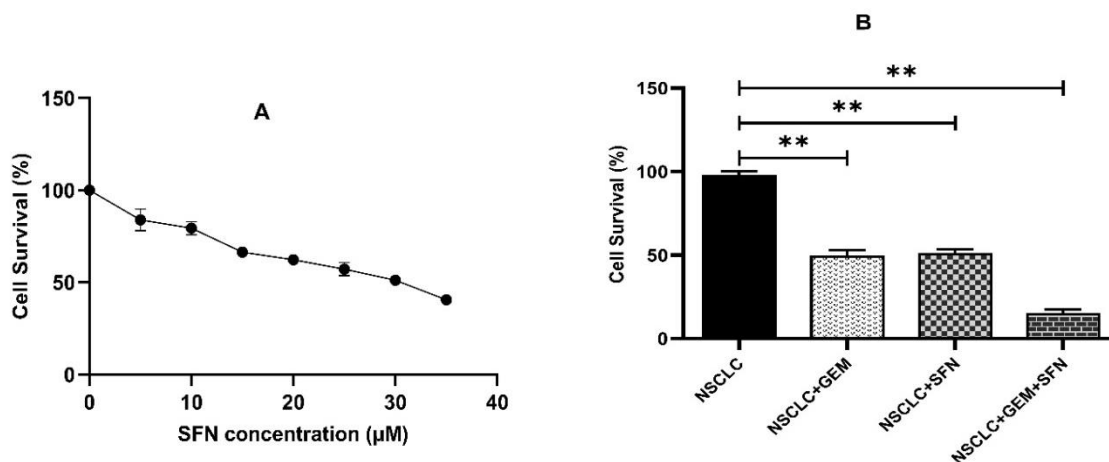


Fig. 1. *In vitro* studies on A549 human cell line. (A) Anticancer effect of different concentrations of SFN against A549 cells. (B) Cellular growth inhibition effect of SFN and/or GEM on A549 cells. Error bars represent means + standard deviation (SD). ** means that the p -value < 0.001. The mean difference is significant at p -value less than 0.05 and is highly significant at p -value less than 0.001.

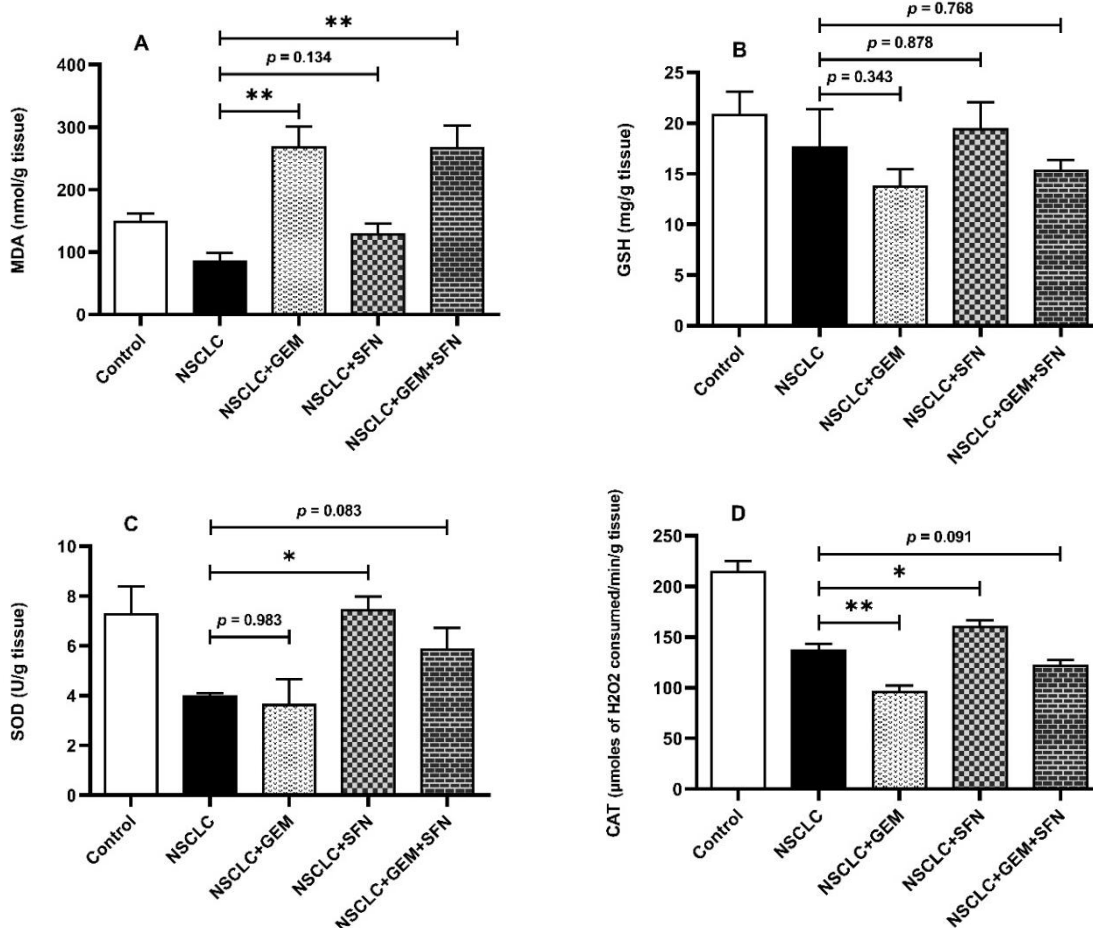


Fig. 2. The effect of GEM, SFN, and GEM+SFN on oxidative status in the NSCLC rat model. A, B, C, and D represent analyses of the MDA, GSH content, and CAT and SOD activity, respectively. Error bars represent means + standard deviation (SD). (*) means that the p -value < 0.05 and (**) means that the p -value < 0.001. The mean difference is significant at p -value less than 0.05 and is highly significant at p -value less than 0.001.

Compared to NSCLC group, the levels of CD133 manifested a highly significant fall in GEM, SFN, and SFN+GEM treatment groups ($p < 0.001$ for all groups) (Fig. 3d). A highly significant rise of ALDH1A1 level has been found in NSCLC group relative to the normal control group ($p < 0.001$). It has been found that ALDH1A1 levels were lowered in GEM, SFN, and SFN+GEM treatment groups with a highly significant difference from NSCLC group ($p < 0.001$ for all groups) (Fig. 3e).

3.6. Histological alterations in lung tissues induced by GEM, SFN, and GEM+SFN

Lung tissues examination in rats of normal control groups has shown normal lung architecture, thin inter-alveolar septa, folded columnar epithelial cells of bronchiole, clearly viewed alveolar sacs, normal pulmonary vessels, and normal distribution of fibrous tissues. The alveoli appeared inflated with thin inter-alveolar septa. They have been shown to be lined mostly by squamous type I pneumocytes and a few large cuboidal type II pneumocytes (Figure 4A).

The lungs of carcinogenic animals' group (NSCLC group) showed undifferentiated tumor mass typically non-small cell lung carcinoma characterized by moderate nuclear pleomorphism, prominent nucleoli, and a moderate amount of cytoplasm. Central "infarct-like" coagulative necrosis was present with a rim of histiocytes and lymphocytic reaction at the edge of the necrosis. In zones at the edge of the necrosis were macrophages with foamy cytoplasm, cholesterol clefts and multinucleated giant cells (Figure 4B and 4C). Partial obstruction with focal emphysema and focal atelectasis were seen. Desquamation of bronchial epithelial which accompanied with peribronchial and perivascular inflammatory cells infiltration mainly lymphocytes, macrophages and few neutrophils were noticed (Figure 4D).

In GEM group, histological changes seen in pathologic responders circumscribed area of extensive necrosis is seen with a rim of fibrosis, chronic inflammatory infiltrate, and prominent cholesterol clefts. The adjacent to the necrosis showed "foamy" macrophages and cholesterol clefts. Grade I b, morphologic indication of therapy-induced alterations but >10% residual tumor was seen (Figure 4E). The lung tissue section revealed mild thickening of alveolar wall and desquamation of bronchial epithelial lining. Peribronchial and perivascular edema and mononuclear cells infiltration mainly lymphocytes and macrophages were noticed (Figure 4F).

The histological picture of lung tissue section of animals' group treated by SFN not completely varied from untreated group. The responsibility of cancerous mass Grade I b. The neoplastic area showed mixture of foam cells and giant cells, in addition to infarct-like coagulative necrosis and minimal fibrosis. The histological growth pattern of the carcinomas was unchanged by therapy (Figure 4G). The lung tissue section showed multifocal areas of emphysema with thickening of alveolar septa. Perivascular edema and massive leukocytic infiltration mainly lymphocytes, macrophages and few neutrophils were seen (Figure 4H).

Lung tissue section of animal group treated by GEM+SFN combination therapy revealed shrinkage of tumor mass in comparison with animals group treated by chemotherapy alone. Remnant of necrotic tissues was surrounded by thick layer of fibrous connective tissues. Chronic inflammatory cells infiltration mainly lymphocytes and macrophages with few cholesterol clefts were seen. Grade II a, extensive response but with residual tumor < 10% was recorded (Figure 4I). A normal histological structure has been shown in the lung tissue section. Peribronchial and perivascular edema and mononuclear cells infiltration mainly lymphocytes and macrophages have been observed (Figure 4J).

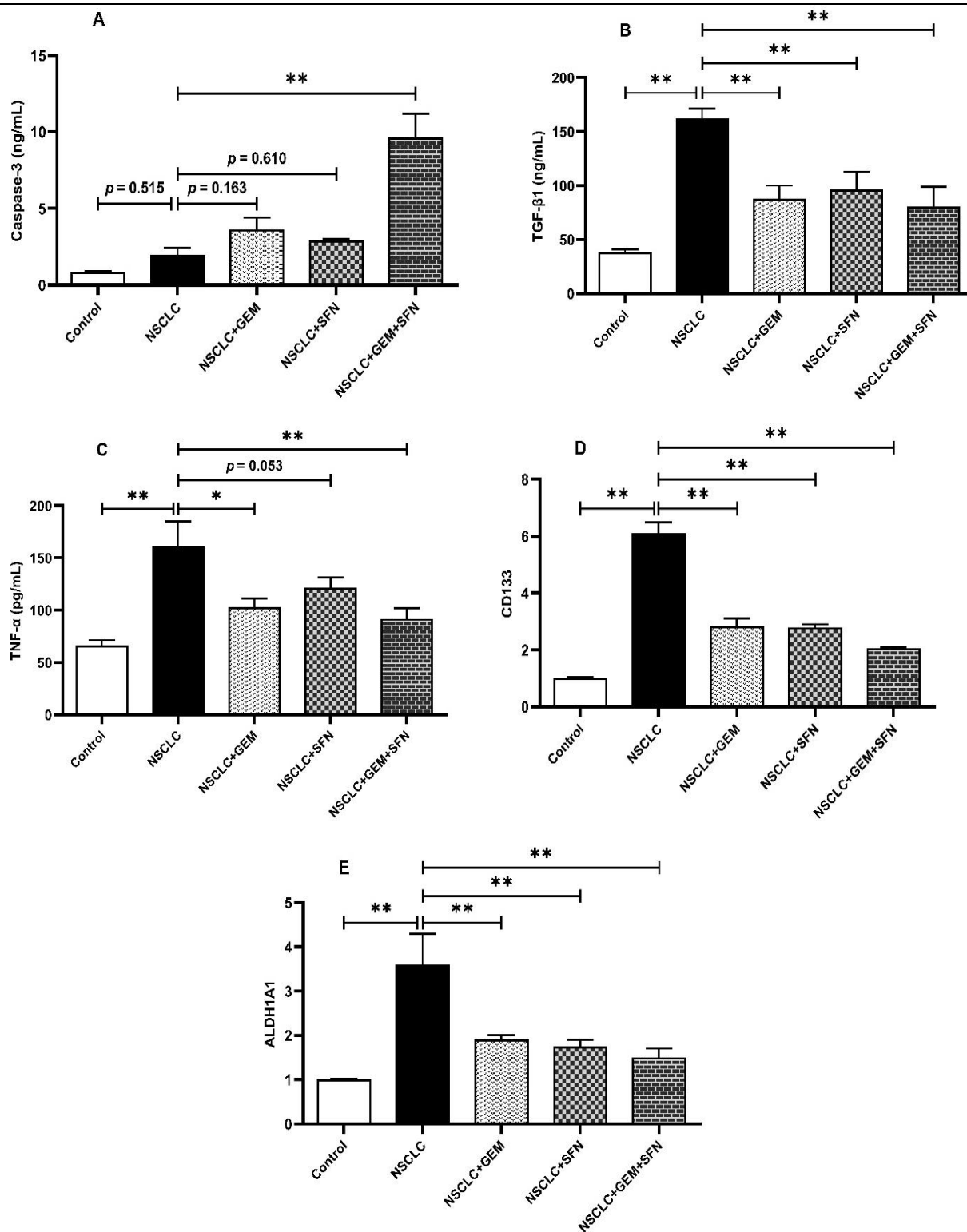
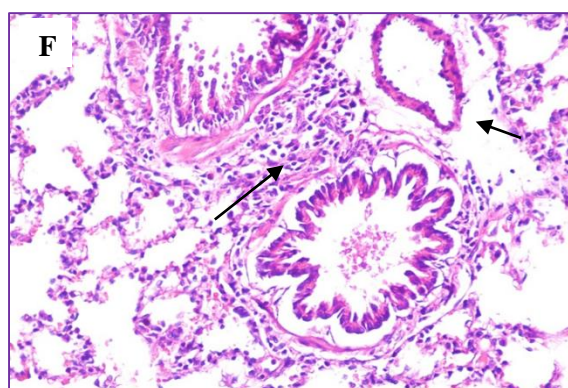
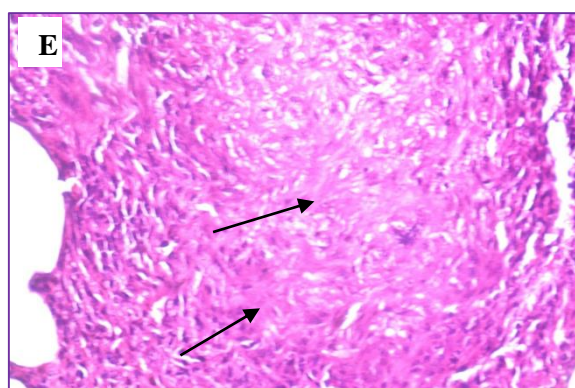
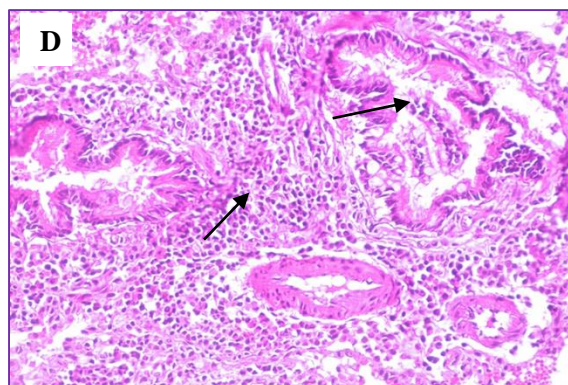
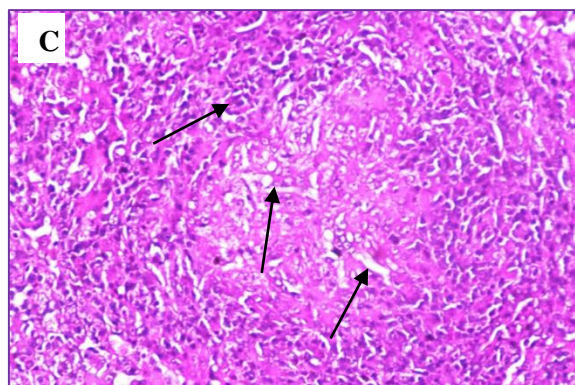
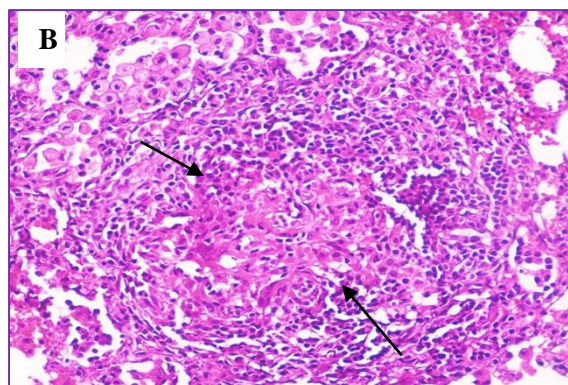
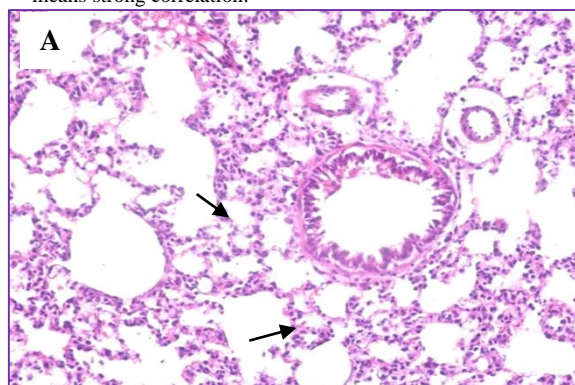


Fig. 3. The effect of SFN, GEM, and SFN+GEM on apoptosis, and on lung CSCs markers via targeting both TGF-β1 and TNF-α in NSCLC rat model. (A, B and C) ELISA analyses of caspase-3, TGF-β1 and TNF-α, respectively. (D and E) qRT-PCR analyses of the lung CSCs markers, CD133 and ALDH1A1, respectively. Error bars represent means + SD. (*) means that the p -value < 0.05 and (**) means that the p -value < 0.001. The mean difference is significant at p -value less than 0.05 and is highly significant at p -value less than 0.001.

Table 2 Pearson correlation between TGF- β 1, TNF- α , CD133 and ALDH1A1) in NSCLC rat model. A strong correlation between TGF- β 1 and TNF- α has been observed ($r = 0.922, p < 0.001$) indicating their synergistic action that leads to increasing CSCs population in NSCLC.

| | | TGF- β 1 | TNF- α | CD133 | ALDH1A1 |
|--------------------------------|-----------------------------|----------------|---------------|---------|---------|
| TGF-β1 | Pearson Correlation (r) | 1 | 0.922** | 0.957** | 0.896** |
| | p -value | | < 0.001 | < 0.001 | < 0.001 |
| TNF-α | Pearson Correlation (r) | 0.922** | 1 | 0.911** | 0.860** |
| | p -value | < 0.001 | | < 0.001 | < 0.001 |
| CD133 | Pearson Correlation (r) | 0.957** | 0.911** | 1 | 0.970** |
| | p -value | < 0.001 | < 0.001 | | < 0.001 |
| ALDH1A1 | Pearson Correlation (r) | 0.896** | 0.860** | 0.970** | 1 |
| | p -value | < 0.001 | < 0.001 | < 0.001 | |

** means strong correlation.



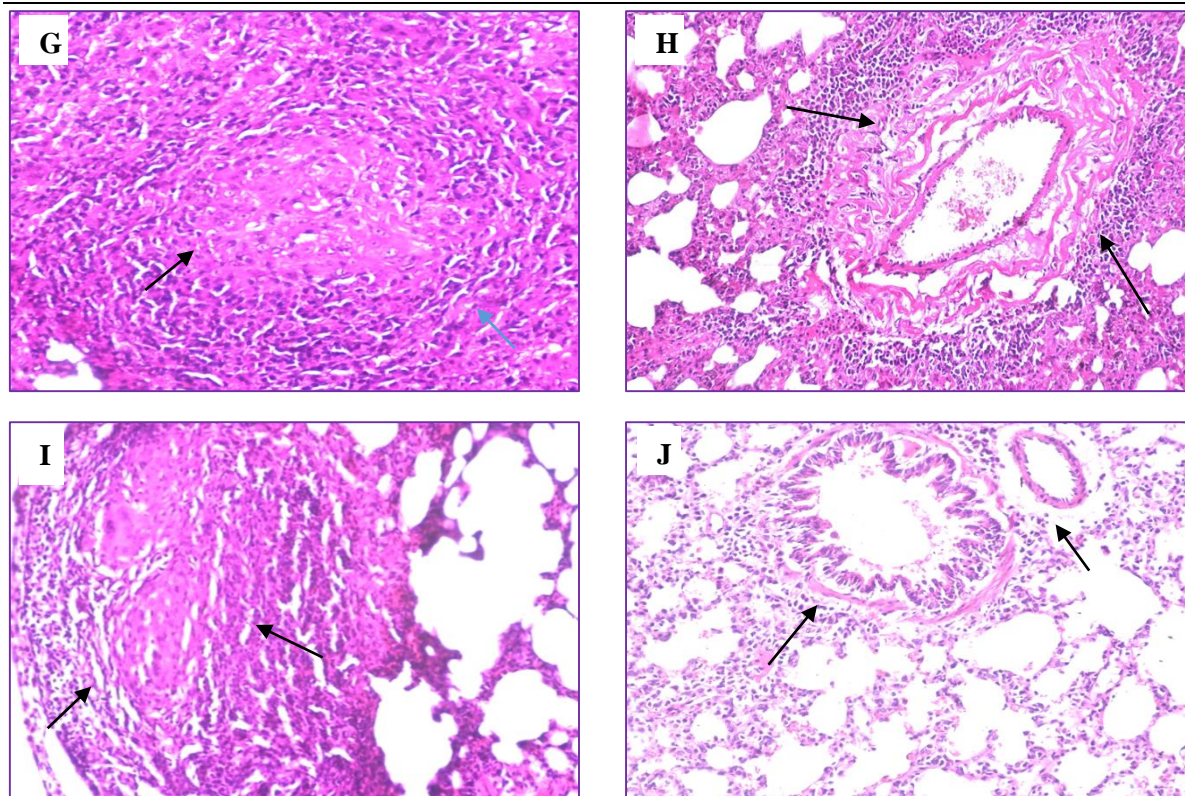


Fig. 4. Histology of lung tissue sections obtained from animals of different groups (H&Ex200). (A) Normal lung tissue section showing thin inter-alveolar septa, folded columnar epithelial cells of bronchiole with normal distribution of pulmonary vessels and fibrous tissue **arrow**. (B) NSCLC tissue section showing central coagulative necrosis with a rim of histiocytes, lymphocytic and foamy macrophage **arrow**. (C) NSCLC tissue section showing central pleomorphic neoplastic cells, cholesterol clefts, **arrow head** and multinucleated giant cell **arrow** (D) NSCLC tissue section showing desquamation of bronchial epithelial accompanied with peribronchial and perivascular inflammatory cells infiltration **arrow**. (E) GEM treated lung tissue section showing extensive necrosis with a rim of fibrosis and chronic inflammatory infiltrate **arrow**. (F) GEM treated lung tissue section showing perivascular edema and mononuclear cells infiltration **arrow**. (G) SFN treated lung tissue section showing a mixture of foam cells, giant cells, in addition to infarct-like coagulative necrosis and rim of fibrosis **arrow**. (H) SFN treated lung tissue section showing perivascular edema and massive leukocytes infiltration, mainly lymphocytes, macrophages, and a few neutrophils **arrow**. (I) GEM+SFN treated lung tissue section showing shrinkage of tumor mass surrounded by thick layer of fibrous connective tissues and chronic inflammatory cells infiltration **arrow**. (J) GEM+SFN treated lung tissue section showing peribronchial and perivascular edema and mononuclear cells infiltration **arrow**.

4. Discussion

The findings reveal that SFN, a natural HDAC blocker, slows resistance induced by chemotherapy GEM in a NSCLC model. The tumor growth of A549 cells was well blocked with GEM+SFN combination therapy than with either drug alone. This might be explained by the ability of GEM to integrate into DNA producing termination of progressive cellular growing through G_{0}/G_{1} phase and S phase arrest which activates apoptosis [40]. It was earlier stated that SFN and broccoli was associated with a decrease in tumor dimensions and development in many rodent cancer models [41,42]. Moreover, SFN and docetaxel combination synergistically increased the shrinkage in the primary tumor and inhibited the metastasis compared with docetaxel alone [43].

Oxidative damage and oxygen radicals destroy DNA through epigenetic modifications, reducing expression of antioxidants such as SOD, causing viral replication, activating growth signaling molecules and the inflammatory factors, and autoimmune reactions that leads to cancer [44–46]. Antioxidants, it can be inferred, inhibit the growth of cancer [47]. In our study, SFN has been revealed to have an antioxidant activity by induction of tissue GSH and SOD and CAT activities associated with reduced MDA content, promoting the elimination of ROS and our finding is in the same line with preceding studies [48, 49].

ROS-dependent angiogenesis is induced by tumor growth which raises caloric intake resulting in elevated ROS levels that lead to stimulation of

growth factors like TGF- β , cytokines (e.g., TNF- α) and transcription factors, which endorse mobility of tumors and spread through ROS-dependent cellular signaling [50]. Consistent with these previous studies, our results have demonstrated that both TGF- β 1 and TNF- α were overexpressed in NSCLC rat model reflecting the crosstalk happened between them and their synergistic action ($r = 0.922$, $p < 0.001$) (Table 2).

NSCLC has been treated with GEM which is an effective chemotherapy with acceptable toxicity profile [51]. However, GEM can cause myelosuppression, the main dose-limiting toxicity of GEM, [51] and has the ability to induce metabolic reprogramming towards aerobic glycolysis and, so, to promote cancer stemness and chemoresistance through the activation of the KRAS/AMPK pathway mediated by ROS as previously demonstrated [11]. CSCs have been reported by several studies to contribute to drug resistance and cancer recurrence. Evidently, CSCs show more resistance against conventional cancer therapies than non-CSCs [52]. Based on these findings and seeking for a way to overcome NSCLC resistance and recurrence, our study has been designed in order to assess the antitumor activity of SFN in treatment of NSCLC by investigating its antiapoptotic activity as well as investigating its antimetastatic effect and anti-CSCs activity via targeting both TGF- β and TNF- α pathways. In compatibility with previous studies [53,54], our data has shown that caspase 3 level was elevated in NSCLC rat model as a result of treatment by SFN as well as GEM. However, the GEM+SFN combination therapy gave better results as it significantly raised the level of caspase 3, thereby, inducing apoptosis of NSCLC model to a significant extent (Figure 3a). Moustafa et al. [55] have found that GEM-induced cell growth inhibition was via ROS generation cytotoxicity and enhanced mitochondrial permeability of the membrane that promotes apoptosis.

TGF- β has been reported to enhance the tumorigenic potential of the CD133⁺ population *in vivo* in hepatocellular carcinoma (HCC) by upregulating the expression of the CSC marker CD133 through a Smad-dependent transcriptional mechanism and via promoting the demethylation of *CD133* promoter since TGF- β negatively affects the DNA methyltransferases DNMT1 and DNMT3 β [56,57]. Moreover, TGF- β triggers

EMT, which is often associated with stemness characteristics acquisition in lung cancer, promoting thereby tumor invasion and metastasis [58–60]. Also, it has been reported that crosstalk occurs between TGF- β and TNF- α , positively affecting the acquisition of a CSCs phenotype in breast cancer as a result of EMT induction and consequently increasing tumorigenicity and chemotherapy drug resistance [22]. The upregulation of CD133 and ALDH1A1 (Figure 3d, e) could be due to increased TGF- β /TNF- α levels (Figure 3b, c). It has been reported that TGF- β 1 is upregulated by TNF- α via a complex mechanism including both increased transcription and mRNA stability [61]. The upregulated results in CD133 and ALDH1A1 mRNA in NSCLC cells indicating the encouraging effect of TGF- β 1 and TNF- α on CSCs increasing their population and might contribute to NSCLC resistance to gemcitabine treatment. Upon treatment using SFN or GEM, TGF- β 1 level has been decreased significantly in NSCLC rat group, as well TNF- α level has been lowered. Furthermore, the expression of both CD133 and ALDH1A1 has been significantly downregulated denoting that CSCs population was significantly reduced. The GEM+SFN combination therapy, compared to GEM and SFN monotherapies, has shown an improved potential to reduce both TGF- β 1 and TNF- α levels, thus decreasing CSCs population reflected by lowering CD133 and ALDH1A1 levels. The reduction of the level of CSCs-related markers and signaling pathways of several tumors has been shown in sulforaphane in addition to other phytochemicals such as curcumin, *epigallocatechin gallate* (EGCG), Lycopene, *Resveratrol*, SR-T100, various flavonoids, *Wisteria floribunda agglutinine* (WFA), Wogonin, *W. somnifera* and Genistein derivatives [62,63].

Remarkably, SFN opposes gefitinib tolerance in human A549 cells via the Sonic Hedgehog signaling modulation [64] and controls the self-renewal of CSCs in pancreatitis [65]. Additionally, SFN confirmed a blocker result on gastrointestinal CSCs [66]. SFN has been reported to lower associated purine metabolites and amino acids in (MCF-7) breast cancer cells, offering a new understanding of the possible process through which it may function as an agent for cancer chemoprevention [67].

Our findings have proved that our therapies, SFN and especially the combination therapy, were significantly efficacious in treatment of NSCLC and

overcoming its resistance and recurrence. Although the GEM+SFN combination therapy has manifested greater effectiveness than both GEM and SFN monotherapies, SFN monotherapy was able to reduce the oxidative stress in NSCLC cells and in turn minimize ROS-related side effects including cancer stemness and chemoresistance at a time when neither GEM nor the GEM+SFN combination therapy could achieve this. Our results have been confirmed by the histological examinations.

5. Conclusions

From our results, it has been found that sulforaphane inhibited CSCs development and enhanced the therapeutic efficacy of GEM in NSCLC. Additionally, SFN exerted its antioxidant activity and anti-metastatic effects. The greatest results have been obtained through the combination of gemcitabine and sulforaphane (GEM+SFN combination therapy), the use of which may help overcome NSCLC resistance and recurrence, the primary concern regarding NSCLC. However, it turns out that the combination therapy did not reduce oxidative stress as sulforaphane monotherapy, hence we recommend that it may be effective in the case of a controlled programmed reduction in the dose of gemcitabine and a controlled programmed increase in the dose of sulforaphane.

6. Ethics approval

The National Institutes of Health's Guide for the Care and Use of Laboratory Animals (NIH Publication No. 85-23, revised 1996) were followed by all ethical protocols for animal treatment, with approval number HU. IACUC.BioChem. / MO-11/08/19 and supervised by the animal facilities, National Center for Radiation Research and Technology, Egyptian Atomic Energy Authority.

7. Conflicts of interest

There are no conflicts to declare.

8. Formatting of funding sources

The authors did not receive any funding for the research, authorship, and/or publication of this paper.

9. Acknowledgments

Authors gratefully thank Dr. Ahmed Othman (Professor of Histopathology, Faculty of Veterinary Medicine, Cairo University) for performing the histopathological examinations in the current study.

10. References

- [1] WHO. Latest global cancer data: Cancer burden rises to 18.1 million new cases and 9.6 million cancer deaths in 2018. Press Release 2018:13–5.
- [2] Sandler AB, Nemunaitis J, Denham C, Von Pawel J, Cormier Y, Gatzemeier U, et al. Phase III trial of gemcitabine plus cisplatin versus cisplatin alone in patients with locally advanced or metastatic non-small-cell lung cancer. *J Clin Oncol* 2000;18:122–30. <https://doi.org/10.1200/jco.2000.18.1.122>.
- [3] Cardenal F, Paz López-Cabrerizo M, Antón A, Alberola V, Massuti B, Carrato A, et al. Randomized phase III study of gemcitabine-cisplatin versus etoposide-cisplatin in the treatment of locally advanced or metastatic non-small-cell lung cancer. *J Clin Oncol* 1999;17:12–8. <https://doi.org/10.1200/jco.1999.17.1.12>.
- [4] Huang P, Chubb S, Hertel LW, Grindey GB, Plunkett W. Action of 2',2'-difluorodeoxycytidine on DNA synthesis. *Cancer Res* 1991;51:6110–7.
- [5] Burris HA, Moore MJ, Andersen J, Green MR, Rothenberg ML, Modiano MR, et al. Improvements in survival and clinical benefit with gemcitabine as first-line therapy for patients with advanced pancreas cancer: A randomized trial. *J Clin Oncol* 1997;15:2403–13. <https://doi.org/10.1200/JCO.1997.15.6.2403>.
- [6] Von der Maase H, Hansen SW, Roberts JT, Dogliotti L, Oliver T, Moore MJ, et al. Gemcitabine and cisplatin versus methotrexate, vinblastine, doxorubicin, and cisplatin in advanced or metastatic bladder cancer: results of a large, randomized, multinational, multicenter, phase III study. *J Clin Oncol* 2000;18:3068–77. <https://doi.org/10.1200/JCO.2000.18.17.3068>.
- [7] Pfisterer J, Plante M, Vergote I, Du Bois A, Hirte H, Lacave AJ, et al. Gemcitabine plus carboplatin compared with carboplatin in patients with platinum-sensitive recurrent ovarian cancer: An intergroup trial of the AGO-OVAR, the NCIC CTG, and the EORTC GCG. *J Clin Oncol* 2006;24:4699–707. <https://doi.org/10.1200/JCO.2006.06.0913>.
- [8] Brodowicz T, Krzakowski M, Zwitter M, Tzekova V, Ramlau R, Ghilezan N, et al. Cisplatin and gemcitabine first-line chemotherapy followed by maintenance

- gemcitabine or best supportive care in advanced non-small cell lung cancer: A phase III trial. *Lung Cancer* 2006;52:155–63. <https://doi.org/10.1016/j.lungcan.2006.01.006>.
- [9] Arora S, Bhardwaj A, Singh S, Srivastava SK, McClellan S, Nirodi CS, et al. An undesired effect of chemotherapy: Gemcitabine promotes pancreatic cancer cell invasiveness through reactive oxygen species-dependent, nuclear factor- κ B- and hypoxia-inducible factor 1 α -mediated up-regulation of CXCR4. *J Biol Chem* 2013;288:21197–207. <https://doi.org/10.1074/jbc.M113.484576>.
- [10] Ju HQ, Gocho T, Aguilar M, Wu M, Zhuang ZN, Fu J, et al. Mechanisms of overcoming intrinsic resistance to gemcitabine in pancreatic ductal adenocarcinoma through the redox modulation. *Mol Cancer Ther* 2015;14:788–98. <https://doi.org/10.1158/1535-7163.MCT-14-0420>.
- [11] Zhao H, Wu S, Li H, Duan Q, Zhang Z, Shen Q, et al. ROS/KRAS/AMPK Signaling Contributes to Gemcitabine-Induced Stem-like Cell Properties in Pancreatic Cancer. *Mol Ther - Oncolytics* 2019;14:299–312. <https://doi.org/10.1016/j.omto.2019.07.005>.
- [12] Visvader JE, Lindeman GJ. Cancer stem cells: Current status and evolving complexities. *Cell Stem Cell* 2012;10:717–28. <https://doi.org/10.1016/j.stem.2012.05.007>.
- [13] Kali A, Ostapchuk YO, Belyaev NN. TNF α and TGF β -1 synergistically increase the cancer stem cell properties of MiaPaCa-2 cells. *Oncol Lett* 2017;14:4647–58. <https://doi.org/10.3892/OL.2017.6810>.
- [14] Hermann PC, Huber SL, Herrler T, Aicher A, Ellwart JW, Guba M, et al. Distinct Populations of Cancer Stem Cells Determine Tumor Growth and Metastatic Activity in Human Pancreatic Cancer. *Cell Stem Cell* 2007;1:313–23. <https://doi.org/10.1016/j.stem.2007.06.002>.
- [15] Xie M, He C, Wei S. Relationship between expression of TGF- β 1, Smad2, Smad4 and prognosis of patients with resected non-small cell lung cancer. *Chinese J Lung Cancer* 2015;18:543–8. <https://doi.org/10.3779/j.issn.1009-3419.2015.09.03>.
- [16] Zhang S, Che D, Yang F, Chi C, Meng H, Shen J, et al. Tumor-associated macrophages promote tumor metastasis via the TGF- β /SOX9 axis in non-small cell lung cancer. *Oncotarget* 2017;8:99801–15. <https://doi.org/10.18632/oncotarget.21068>.
- [17] Vázquez PF, Carlini MJ, Daroqui MC, Colombo L, Dalurzo ML, Smith DE, et al. TGF- β specifically enhances the metastatic attributes of murine lung adenocarcinoma: Implications for human non-small cell lung cancer. *Clin Exp Metastasis* 2013;30:993–1007. <https://doi.org/10.1007/s10585-013-9598-1>.
- [18] Okayama A, Miyagi Y, Oshita F, Ito H, Nakayama H, Nishi M, et al. Identification of Tyrosine-Phosphorylated Proteins Upregulated during Epithelial-Mesenchymal Transition Induced with TGF- β . *J Proteome Res* 2015;14:4127–36. <https://doi.org/10.1021/acs.jproteome.5b00082>.
- [19] Takanami I, Tanaka F, Hashizume T, Kikuchi K, Yamamoto Y, Yamamoto T, et al. Transforming growth factor- β isoforms expressions in pulmonary adenocarcinomas as prognostic markers. *Oncol* 1997;54:122–8. <https://doi.org/10.1159/000227675>.
- [20] Mariathasan S, Turley SJ, Nickles D, Castiglioni A, Yuen K, Wang Y, et al. TGF β attenuates tumour response to PD-L1 blockade by contributing to exclusion of T cells. *Nature* 2018;554:544–8. <https://doi.org/10.1038/nature25501>.
- [21] Varfolomeev EE, Ashkenazi A. Tumor Necrosis Factor: An Apoptosis JuNKie? *Cell* 2004;116:491–7. [https://doi.org/10.1016/S0092-8674\(04\)00166-7](https://doi.org/10.1016/S0092-8674(04)00166-7).
- [22] Asiedu MK, Ingle JN, Behrens MD, Radisky DC, Knutson KL. TGF β /TNF α -mediated epithelial-mesenchymal transition generates breast cancer stem cells with a claudin-low phenotype. *Cancer Res* 2011;71:4707–19. <https://doi.org/10.1158/0008-5472.CAN-10-4554>.

- [23] Balkwill F. TNF- α in promotion and progression of cancer. *Cancer Metastasis Rev* 2006;25:409–16. <https://doi.org/10.1007/s10555-006-9005-3>.
- [24] Ikushima H, Miyazono K. TGF β signalling: a complex web in cancer progression. *Nat Rev Cancer* 2010;10:415–24. <https://doi.org/10.1038/nrc2853>.
- [25] Bayat Mokhtari R, Baluch N, Homayouni TS, Morgatskaya E, Kumar S, Kazemi P, et al. The role of Sulforaphane in cancer chemoprevention and health benefits: a mini-review. *J Cell Commun Signal* 2018;12:91–101. <https://doi.org/10.1007/s12079-017-0401-y>.
- [26] Jabbarzadeh Kaboli P, Afzalipour Khoshkbejari M, Mohammadi M, Abiri A, Mokhtarian R, Vazifemand R, et al. Targets and mechanisms of sulforaphane derivatives obtained from cruciferous plants with special focus on breast cancer – contradictory effects and future perspectives. *Biomed Pharmacother* 2020;121. <https://doi.org/10.1016/j.biopha.2019.109635>.
- [27] Mosmann T. Rapid colorimetric assay for cellular growth and survival: Application to proliferation and cytotoxicity assays. *J Immunol Methods* 1983;65:55–63. [https://doi.org/10.1016/0022-1759\(83\)90303-4](https://doi.org/10.1016/0022-1759(83)90303-4).
- [28] Li J, Pan YY, Zhang Y. Synergistic interaction between sorafenib and gemcitabine in EGFR-TKI-sensitive and EGFR-TKI-resistant human lung cancer cell lines. *Oncol Lett* 2013;5:440–6. <https://doi.org/10.3892/ol.2012.1017>.
- [29] Janker F, Weder W, Jang JH, Jungraithmayr W. Preclinical, non-genetic models of lung adenocarcinoma: A comparative survey. *Oncotarget* 2018;9:30527–38. <https://doi.org/10.18632/oncotarget.25668>.
- [30] Guyer MF, Claus PE. Tumor of the Lung in Rats Following Injections of Urethane (Ethyl Carbamate). *Cancer Res* 1947;7:342–5.
- [31] Clouser CL, Holtz CM, Mullett M, Crankshaw DL, Briggs JE, Chauhan J, et al. Analysis of the ex vivo and in vivo antiretroviral activity of gemcitabine. *PLoS One* 2011;6. <https://doi.org/10.1371/journal.pone.0015840>.
- [32] Yang M, Wang H, Zhou M, Liu W, Kuang P, Liang H, et al. The natural compound sulforaphane, as a novel anticancer reagent, targeting PI3K-AKT signaling pathway in lung cancer. *Oncotarget* 2016;7:76656–66. <https://doi.org/10.18632/oncotarget.12307>.
- [33] Yoshioka T, Kawada K, Shimada T, Mori M. Lipid peroxidation in maternal and cord blood and protective mechanism against activated-oxygen toxicity in the blood. *Am J Obstet Gynecol* 1979;135:372–6. [https://doi.org/10.1016/0002-9378\(79\)90708-7](https://doi.org/10.1016/0002-9378(79)90708-7).
- [34] Ahmed AE, Hussein GI, Loh J -P, Abdel-Rahman SZ. Studies on the mechanism of haloacetonitrile-induced gastrointestinal toxicity: Interaction of dibromoacetonitrile with glutathione and glutathione-S-transferase in rats. *J Biochem Toxicol* 1991;6:115–21. <https://doi.org/10.1002/jbt.2570060205>.
- [35] Minami M, Yoshikawa H. A simplified assay method of superoxide dismutase activity for clinical use. *Clin Chim Acta* 1979;92:337–42. [https://doi.org/10.1016/0009-8981\(79\)90211-0](https://doi.org/10.1016/0009-8981(79)90211-0).
- [36] Sinha AK. Colorimetric assay of catalase. *Anal Biochem* 1972;47:389–94. [https://doi.org/10.1016/0003-2697\(72\)90132-7](https://doi.org/10.1016/0003-2697(72)90132-7).
- [37] Livak KJ, Schmittgen TD. Analysis of relative gene expression data using real-time quantitative PCR and the 2- $\Delta\Delta$ CT method. *Methods* 2001;25:402–8. <https://doi.org/10.1006/meth.2001.1262>.
- [38] Bancroft JD, Stevens A, Turner DR. Theory and Practice of Histological Techniques. 4th editio. New York: Churchill Livingstone; 1996.
- [39] Junker K, Langner K, Klinke F, Bosse U, Thomas M. Grading of tumor regression in non-small cell lung cancer: Morphology and prognosis. *Chest* 2001;120:1584–91. <https://doi.org/10.1378/chest.120.5.1584>.
- [40] Rizzuto I, Ghazaly E, Peters GJ. Pharmacological factors affecting accumulation of gemcitabine's active metabolite, gemcitabine triphosphate. *Pharmacogenomics* 2017;18:911–25. <https://doi.org/10.2217/pgs-2017-0034>.
- [41] Justin S, Rutz J, Maxeiner S, Chun FKH, Juengel E, Blaheta RA. Chronic sulforaphane administration inhibits resistance to the mtor-inhibitor everolimus in bladder cancer cells. *Int J Mol Sci* 2020;21:4026. <https://doi.org/10.3390/ijms21114026>.
- [42] Traka MH, Melchini A, Coode-Bate J, Kadhi O Al, Saha S, Defernez M, et al. Transcriptional changes in prostate of men on active surveillance

- after a 12-mo glucoraphanin-rich broccoli intervention—results from the Effect of Sulforaphane on prostate CAncer PrEvention (ESCAPE) randomized controlled trial. *Am J Clin Nutr* 2019;109:1133–44. <https://doi.org/10.1093/ajcn/nqz012>.
- [43] Cao S, Wang L, Zhang Z, Chen F, Wu Q, Li L. Sulforaphane-induced metabolomic responses with epigenetic changes in estrogen receptor positive breast cancer cells. *FEBS Open Bio* 2018;8:2022–34. <https://doi.org/10.1002/2211-5463.12543>.
- [44] Hernández JA, López-Sánchez RC, Rendón-Ramírez A. Lipids and Oxidative Stress Associated with Ethanol-Induced Neurological Damage. *Oxid Med Cell Longev* 2016;2016. <https://doi.org/10.1155/2016/1543809>.
- [45] Gjorgjieva M, Mithieux G, Rajas F. Hepatic stress associated with pathologies characterized by disturbed glucose production. *Cell Stress* 2019;3:86–99. <https://doi.org/10.15698/cst2019.03.179>.
- [46] Yoon JH, Kim O, Nam SW, Lee JY, Park WS. NKX6.3 Regulates reactive oxygen species production by suppressing NF- κ B and DNMT1 activities in gastric epithelial cells. *Sci Rep* 2017;7. <https://doi.org/10.1038/s41598-017-02901-y>.
- [47] Jabbarzadeh Kaboli P, Rahmat A, Ismail P, Ling KH. Targets and mechanisms of berberine, a natural drug with potential to treat cancer with special focus on breast cancer. *Eur J Pharmacol* 2014;740:584–95. <https://doi.org/10.1016/j.ejphar.2014.06.025>.
- [48] Juge N, Mithen RF, Traka M. Molecular basis for chemoprevention by sulforaphane: A comprehensive review. *Cell Mol Life Sci* 2007;64:1105–27. <https://doi.org/10.1007/s00018-007-6484-5>.
- [49] Ruhee RT, Ma S, Suzuki K. Protective effects of sulforaphane on exercise-induced organ damage via inducing antioxidant defense responses. *Antioxidants* 2020;9:136. <https://doi.org/10.3390/antiox9020136>.
- [50] Dewhirst MW, Cao Y, Moeller B. Cycling hypoxia and free radicals regulate angiogenesis and radiotherapy response. *Nat Rev Cancer* 2008;8:425–37. <https://doi.org/10.1038/nrc2397>.
- [51] Toschi L, Cappuzzo F. Gemcitabine for the treatment of advanced nonsmall cell lung cancer. *Oncotargets Ther* 2009;2:209–17. <https://doi.org/10.2147/ott.s4645>.
- [52] Chen K, Huang YH, Chen JL. Understanding and targeting cancer stem cells: Therapeutic implications and challenges. *Acta Pharmacol Sin* 2013;34:732–40. <https://doi.org/10.1038/aps.2013.27>.
- [53] Park SY, Kim GY, Bae SJ, Yoo YH, Choi YH. Induction of apoptosis by isothiocyanate sulforaphane in human cervical carcinoma HeLa and hepatocarcinoma HepG2 cells through activation of caspase-3. *Oncol Rep* 2007;18:181–7. <https://doi.org/10.3892/or.18.1.181>.
- [54] Yong-Xian G, Xiao-Huan L, Fan Z, Guo-Fang T. Gemcitabine inhibits proliferation and induces apoptosis in human pancreatic cancer PANC-1 cells. *J Cancer Res Ther* 2016;12:C1–4. <https://doi.org/10.4103/0973-1482.191615>.
- [55] Moustafa EM, Rashed LA, El-Sebaie MM, Thabet NM, Abdel-Rafei MK. Crosstalk between ER-stress and apoptosis in irradiated HepG2 cells with gemcitabine: implication of PI3K/AKT and I κ B/NF- κ B signaling pathways. *J Radiat Res Appl Sci* 2020;13:144–54. <https://doi.org/10.1080/16878507.2020.1715569>.
- [56] Wang XH, Liu MN, Sun X, Xu CH, Liu J, Chen J, et al. TGF- β 1 pathway affects the protein expression of many signaling pathways, markers of liver cancer stem cells, cytokeratins, and TERT in liver cancer HepG2 cells. *Tumor Biol* 2016;37:3675–81. <https://doi.org/10.1007/s13277-015-4101-z>.
- [57] You H, Ding W, Rountree CB. Epigenetic regulation of cancer stem cell marker CD133 by transforming growth factor- β . *Hepatology* 2010;51:1635–44. <https://doi.org/10.1002/hep.23544>.
- [58] Lee SH, Shin JH, Shin MH, Kim YS, Chung KS, Song JH, et al. The effects of retinoic acid and MAPK inhibitors on phosphorylation of Smad2/3 induced by transforming growth factor β 1.

- Tuberc Respir Dis (Seoul) 2019;82:42–52. <https://doi.org/10.4046/trd.2017.0111>.
- [59] Katsuno Y, Lamouille S, Derynck R. TGF- β signaling and epithelial-mesenchymal transition in cancer progression. *Curr Opin Oncol* 2013;25:76–84. <https://doi.org/10.1097/CCO.0b013e32835b6371>.
- [60] Kim BN, Ahn DH, Kang N, Yeo CD, Kim YK, Lee KY, et al. TGF- β induced EMT and stemness characteristics are associated with epigenetic regulation in lung cancer. *Sci Rep* 2020;10. <https://doi.org/10.1038/s41598-020-67325-7>.
- [61] Sullivan DE, Ferris M, Nguyen H, Abboud E, Brody AR. TNF- α induces TGF- β 1 expression in lung fibroblasts at the transcriptional level via AP-1 activation. *J Cell Mol Med* 2009;13:1866–76. <https://doi.org/10.1111/j.1582-4934.2009.00647.x>.
- [62] Singh AK, Sharma N, Ghosh M, Park YH, Jeong DK. Emerging importance of dietary phytochemicals in fight against cancer: Role in targeting cancer stem cells. *Crit Rev Food Sci Nutr* 2017;57:3449–63. <https://doi.org/10.1080/10408398.2015.1129310>.
- [63] Moustafa EM, Abdel Salam HS, Mansour SZ. *Withania somnifera* modulates radiation-induced generation of lung cancer stem cells via restraining the hedgehog signaling factors. *Dose Response*. 2022;24;20(1):15593258221076711.
- [64] Wang F, Wang W, Li J, Zhang J, Wang X, Wang M. Sulforaphane reverses gefitinib tolerance in human lung cancer cells via modulation of sonic hedgehog signaling. *Oncol Lett* 2018;15:109–14. <https://doi.org/10.3892/ol.2017.7293>.
- [65] Rodova M, Fu J, Watkins DN, Srivastava RK, Shankar S. Sonic Hedgehog Signaling Inhibition Provides Opportunities for Targeted Therapy by Sulforaphane in Regulating Pancreatic Cancer Stem Cell Self-Renewal. *PLoS One* 2012;7. <https://doi.org/10.1371/journal.pone.0046083>.
- [66] Ge M, Zhang L, Cao L, Xie C, Li X, Li Y, et al. Sulforaphane inhibits gastric cancer stem cells via suppressing sonic hedgehog pathway. *Int J Food Sci Nutr* 2019;70:570–8. <https://doi.org/10.1080/09637486.2018.154501>
- [67] Aumeeruddy MZ, Mahomoodally MF. Combating breast cancer using combination therapy with 3 phytochemicals: Piperine, sulforaphane, and thymoquinone. *Cancer* 2019;125:1600–11. <https://doi.org/10.1002/cncr.32022>.